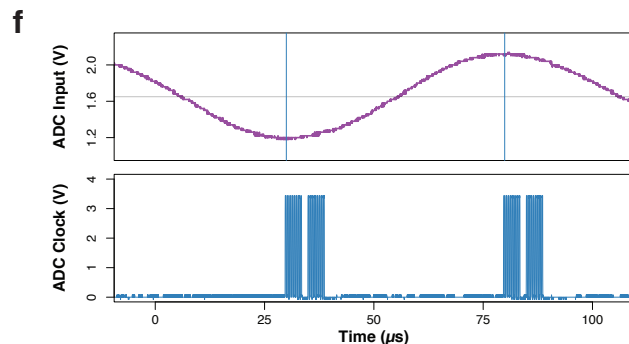
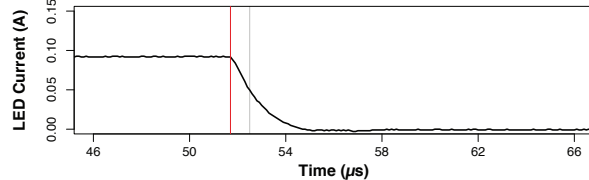
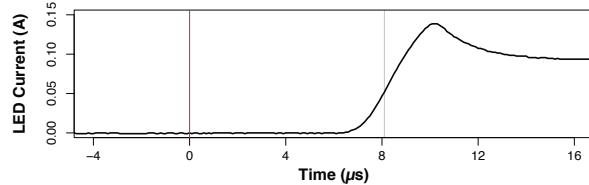
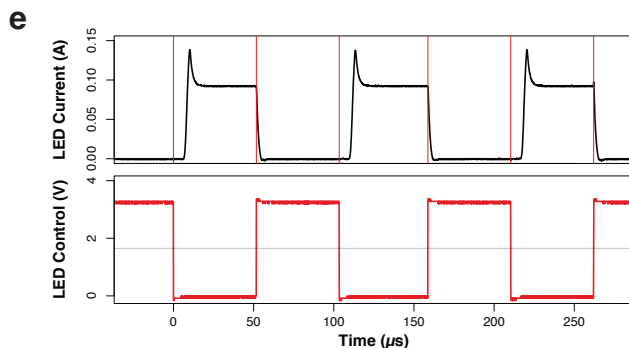
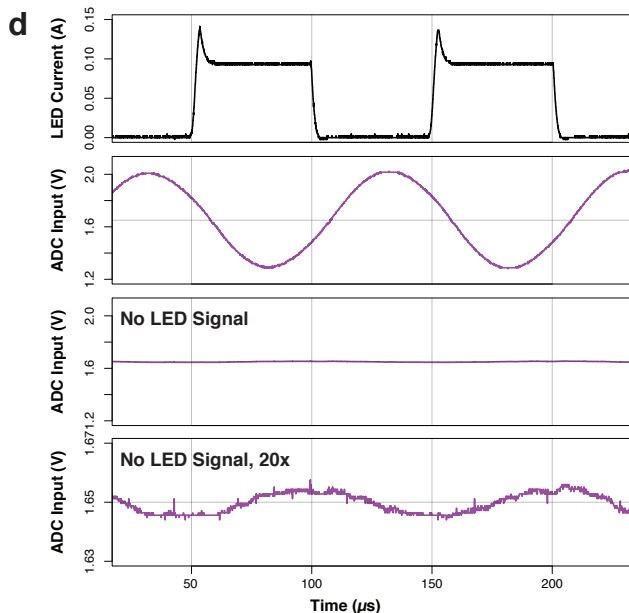
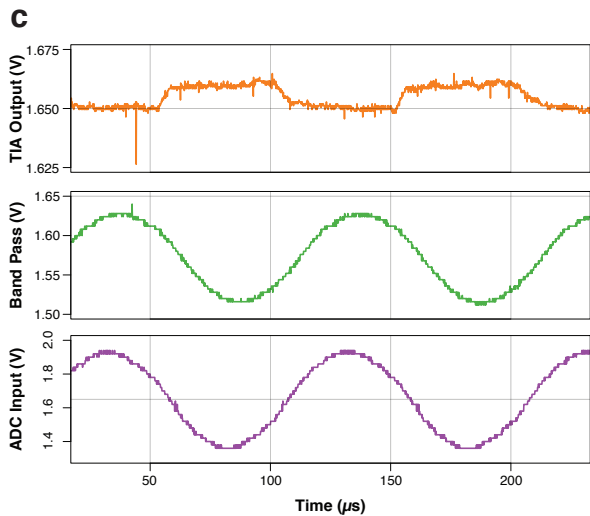
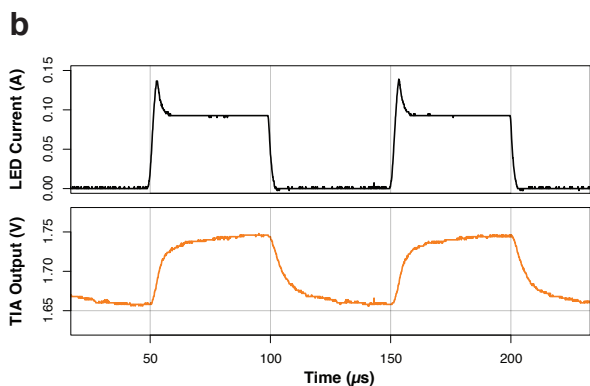
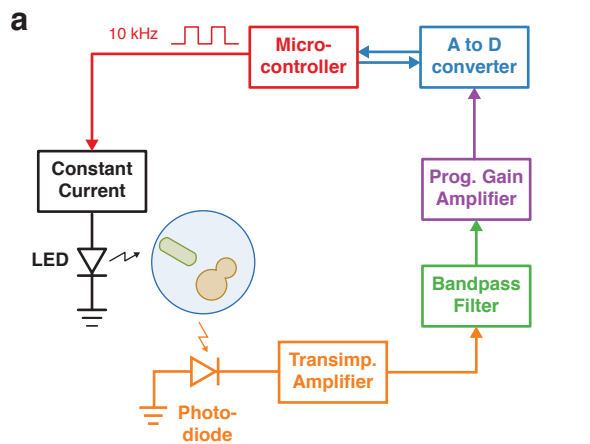


# Supplementary Figure 1



**Supplementary Figure 1. A synchronous detector that measures scattered light intensity against high ambient background.**

(a) Diagram of synchronous detector design. A microcontroller modulates LED illumination and measures the scattered light signal at an optimized phase relative to the LED.

Scattered light is detected by a photodiode and transimpedance amplifier (TIA), and this signal is filtered to extract the 10 kHz signal from ambient light and electronic noise. (b) Response of the photodiode/TIA to a 10 kHz square wave of strong illumination. The detector bandwidth of  $\sim 200$  kHz captures the illumination profile. Faint vertical lines indicate LED switching and faint horizontal lines indicate the 1.65V virtual ground.

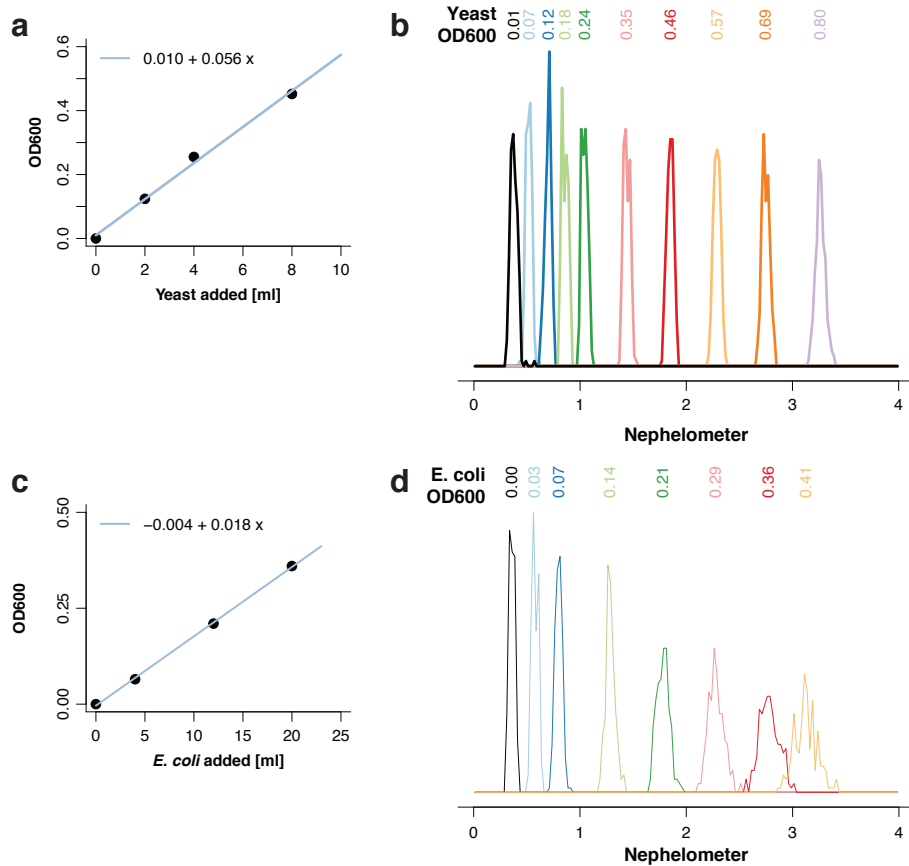
(c) Filtering and amplification of weak illumination. The 10 kHz bandpass filter (BPF) extracts a sinusoidal signal with 10x inverted gain and the programmable gain amplifier (PGA) provides an additional 5x non-inverting gain. Faint vertical lines indicate LED switching and faint horizontal lines indicate the 1.65V virtual ground.

(d) Overall response of detector and filter to a 10 kHz square wave of weak illumination. When LED illumination is suppressed, a faint background signal can be observed in a different phase relative to the LED driver. This  $< 10$  mV signal reflects the noise floor of the detector.

Faint vertical lines indicate LED switching and faint horizontal lines indicate the 1.65V virtual ground. (e) The LED controller has an asymmetric switching delay. LED current switches on  $\sim 8$   $\mu$ s after the control signal activates, and switches off  $\sim 1$   $\mu$ s after the control signal deactivates. Vertical red lines indicate the times of control switching and faint vertical lines indicate the times of LED current switching. (f)

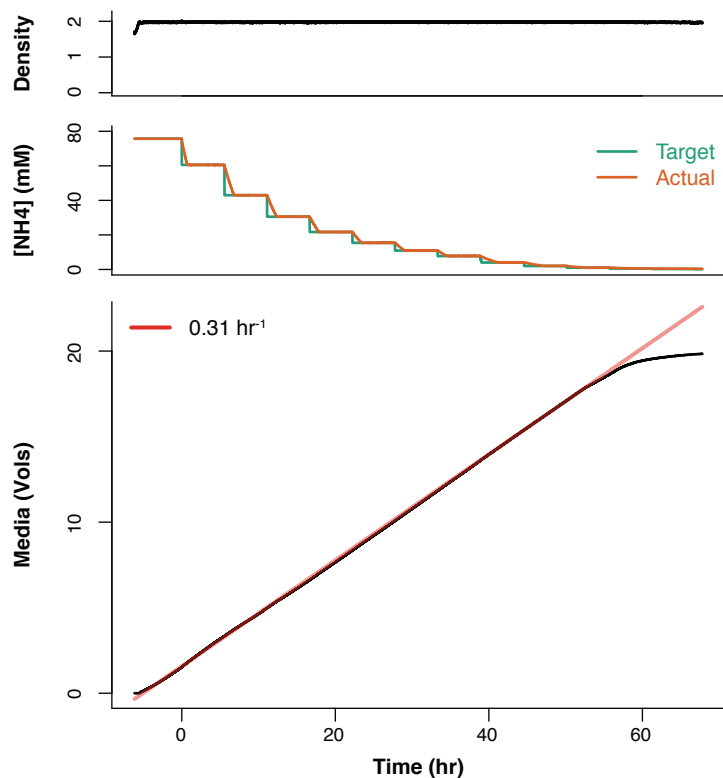
Acquisition timing tuned to the phase delay in the detector circuit. LED illumination was driven by a 10 kHz square wave with 50% duty cycle, accounting for the asymmetric switching described in (e), by activating the control at 0  $\mu$ s and inactivating it at 57  $\mu$ s. Data acquisition by the analog-to-digital converter (ADC) is triggered on the second falling edge of the clock signal provided by the microcontroller. Data was acquired at 30  $\mu$ s and 80  $\mu$ s, which align well with the trough and peak of the analog input signal, providing phase- and frequency-sensitive detection of true scattered light signal against asynchronous background.

## Supplementary Figure 2



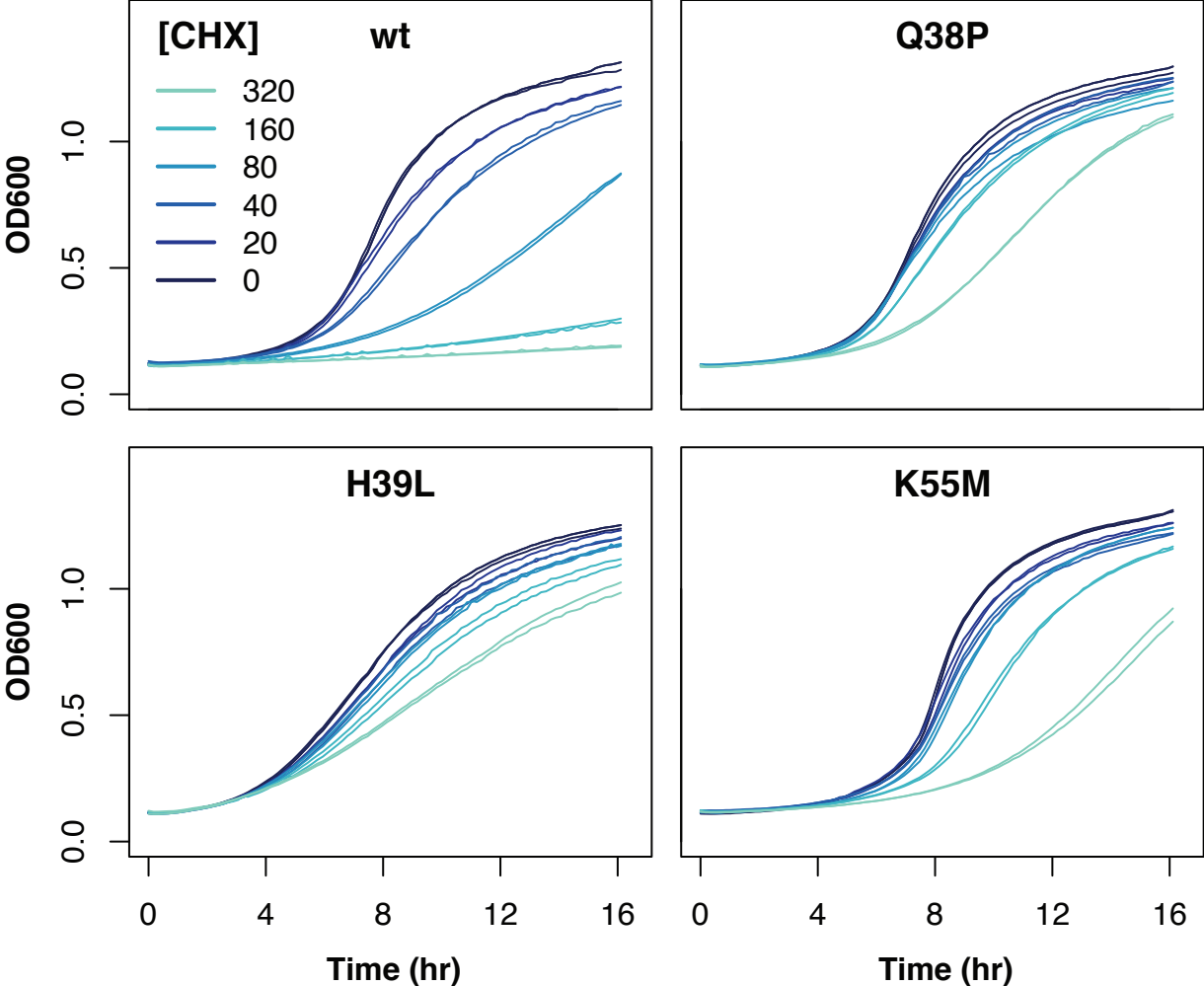
**Supplementary Figure 2. Calibration of cell density, absorbance, and turbidity measurements for yeast and bacteria.** (a) Budding yeast OD600 scales linearly with cell density. (b) Histogram of turbidity measurements at different yeast OD600 values. (c) *E. coli* OD600 scales linearly with cell density. (d) Histogram of turbidity measurements at different *E. coli* OD600 values.

### Supplementary Figure 3



**Supplementary Figure 3. Growth of prototrophic S288c in media with progressively reduced nitrogen.** Cell density, growth medium composition, and cumulative media addition for a turbidostat culture with step-wise reduction in the ammonium composition. The dilution rate, and thus the growth rate, remains constant from the standard 76 mM [NH<sub>4</sub><sup>+</sup>] down below 4 mM [NH<sub>4</sub><sup>+</sup>], but growth ultimately stops at very low nitrogen levels.

Supplementary Figure 4



Supplementary Figure 4. Growth of *RPL28* variants in cycloheximide. Growth curves for individual cultures of NIY414 with *RPL28* variant plasmids are shown.

Table S1: Oligonucleotide sequences

Name	Purpose	Sequence
NI-NI-38	Fragment input library sequencing	CAAGCAGAAGACGGCATAACGAGATCGTCAGGTGACTGGAGTTCAGACGTGTGCTCTTCCG
NI-AM-197	Fragment recombinational cloning	GAAGTAATTATCTACTTTTTACAACAAATTAATTTAAATGACACTCTTTCCCTACACGAC
NI-AM-199	Fragment recombinational cloning	GTTTCTCAGCGCGACGCTCACGTCGTCGTGTTTGTGCGTCGTGACTGGAGTTCAGACGTG
NI-AM-226	Fragment selection library sequencing	GTTTGCAGCTTTCATTGAGCTTGTCTCTCAGC
NI-AM-227	Fragment selection library sequencing	CGTCACACAACAAGGTCCTAGCGACG
NI-AM-228	Fragment selection library sequencing	AATGATACGGCGACCACCGAGATCTACACTCTTTCCTACACGACGCTCTTCCGATCT
NI-NI-3	Fragment selection library sequencing	CAAGCAGAAGACGGCATAACGAGATAGTCGTGACTGGAGTTCAGACGTGTGCTCTTCCG
NI-NI-880	Cloning RPL28(KpnI)	ACAGGCAAGCGATCCGTCGGATCCAAATATGCCACCGTTACC
NI-NI-881	Cloning RPL28(KpnI)	TAATTGCGCTCTCTACAACCATTTGGTACCATACAGCGATAAATTAGTCTTCCATAATC
NI-NI-882	Cloning RPL28(KpnI)	GATTATGGAAGCACTAATTATCGCTGTATGGTACCAATGGTTGTAGAGAGCGCAATTA
NI-NI-883	Cloning RPL28(KpnI)	AATTCGCTTATTTAGAAGTGGCGCGCTTTTAAAAAAGCGATAAAAAGCGTTGG
NI-NI-893	Sequencing RPL28	ACCACACAGAAAATCCTGTGAT
NI-NI-894	Sequencing RPL28	AGGTTCAATCCACCTCGTCTCT
NI-NI-895	Sequencing RPL28	ACACCAGGGACCCACACATTAC
NI-NI-896	Sequencing RPL28	AGCTGATTGACATTTCTCTGTACC
NI-NI-897	Sequencing RPL28	ACTGTCTACTCATTTTACGGCT
NI-NI-898	Sequencing RPL28	TGGTCTCTTGTCTCTGGGA
NI-NI-899	Sequencing RPL28	GCTGCTGGTGGTGTGTGAAT
NI-NI-900	Sequencing RPL28	GGGACGAGGCAAGCTAAACAGA
NI-NI-914	Deleting RPL28	acacaagaataagtatgaggtagtttgctctcgaaaaaaccagctgaagcttcgtacgc
NI-NI-915	Deleting RPL28	CTATGTTTATATATGGATTTGAAAATCTTTTAAAAAagcatagggcactagtgatctg
NI-NI-901	Verifying rpl28Δ::KILEU2	CTAACTCTACCCTGAGGTTGG
NI-NI-905	Verifying rpl28Δ::KILEU2	tgccgccaatataatattaacacac
NI-NI-908	Verifying rpl28Δ::KILEU2	CGCTAACTGATAAATTTGGGTGAGG
NI-NI-912	Verifying rpl28Δ::KILEU2	CAGCGTTTGAATTTGACGAGTC
NI-NI-954	Cloning RPL28 exon 1-(Mfe/Nhe)	agctagcACTTCTAAATAAGCGAATTTTC
NI-NI-955	Cloning RPL28 exon 1-(Mfe/Nhe)	gtcaattgATACAGCGATAAATTAGTGC
NI-NI-886	Mutagenizing RPL28 exon 2	GCACTAATTATCGCTGTATGGTACC
NI-NI-913	Mutagenizing RPL28 exon 2	GCGATAAAAGCGTTGGGATC
NI-NI-952	Mutagenizing RPL28 exon 2	ATACAATTGAAATGGTTGTAGAGAGCGC
NI-NI-953	Mutagenizing RPL28 exon 2	TATGCTAGCACGACGCTCTTCCGATCTNNNNNNNNNNNNNNNGCGATAAAAGCGTTGGG
NI-NI-956	RPL28 barcode counting and genotyping	AATGATACGGCGACCACCGAGATCTACACTCTTTCCTACACGACGCTCTTCCGATC
NI-NI-957	RPL28 barcode genotyping	CAAGCAGAAGACGGCATAACGAGATGTCCTCGTGGGCTCGG
NI-NI-958	RPL28 barcode genotyping	AGATCGCTCGTCGGCAGCGTC
NI-NI-945	RPL28 barcode counting	GTGACTGGAGTTCAGACGTGTGCTCTTCCGATCTGATCCCAACGCTTTTATCGC
NI-NI-798	RPL28 barcode counting	AATGATACGGCGACCACCGAGATCTACACTCTTTCCTACACGACGCTC
NI-NI-799	RPL28 barcode counting	CAAGCAGAAGACGGCATAACGAGATCGTGATGTGACTGGAGTTCAGACGTGTG
NI-NI-951	RPL28 barcode counting	CAAGCAGAAGACGGCATAACGAGATTACAAGGTGACTGGAGTTCAGACGTGTG
NI-NI-999	RPL28 barcode counting	CAAGCAGAAGACGGCATAACGAGATTGTTGACTGTGACTGGAGTTCAGACGTGTG
NI-NI-1000	RPL28 barcode counting	CAAGCAGAAGACGGCATAACGAGATACGGAAGTGTGACTGGAGTTCAGACGTGTG
NI-NI-1001	RPL28 barcode counting	CAAGCAGAAGACGGCATAACGAGATTCTGACATGTGACTGGAGTTCAGACGTGTG
NI-NI-1002	RPL28 barcode counting	CAAGCAGAAGACGGCATAACGAGATCGGGACGGGTGACTGGAGTTCAGACGTGTG
NI-NI-1003	RPL28 barcode counting	CAAGCAGAAGACGGCATAACGAGATGTGCGGACGTGACTGGAGTTCAGACGTGTG
NI-NI-1004	RPL28 barcode counting	CAAGCAGAAGACGGCATAACGAGATCGTTTACAGTGTGACTGGAGTTCAGACGTGTG
NI-NI-1005	RPL28 variant reconstruction	GGAAAGCACTAATTATCGCTGTATcAATTGAAATGGTTGTAGAGAGCGC
NI-NI-1006	RPL28 variant reconstruction	TAAGAAATTCGCTTATTTAGAAGTgctagcGCGATAAAAGCGTTGGGATC

Name	Purpose	Sequence
NI-NI-1007	RPL28 variant reconstruction	GGCCGGTGGTCcACATCACCACAGAATTAACATGG
NI-NI-1008	RPL28 variant reconstruction	TGTGGTGATGTgGACCACCGGCCATACC
NI-NI-1009	RPL28 variant reconstruction	TTATTTTCGGTAtGGTTGGTATGAGATACTCCACAAG
NI-NI-1010	RPL28 variant reconstruction	CATACCAACCATACCgAAATAACCTGGATGGT
NI-NI-1011	RPL28 variant reconstruction	CGGTGGTCAAttgCACCACAGAATTAACATGGATAAATACC
NI-NI-1012	RPL28 variant reconstruction	TTCTGTGGTGcaaTTGACCACCGGCCATACC

**Supplementary Table 1. Oligonucleotide sequences.** Oligonucleotides used in this study are listed along with their sequence. A text version of data in this table is available at <https://github.com/ingolia-lab/turbidostat/tree/master/mcgeachy-2018/sequences>.



## Supplementary Table 2

Plasmid	Description	Reference
pHLUM v2 (pNTI599)	ARS/CEN HIS3 LEU2 URA3 MET17	Müller et al., F1000Res 2016
pNTI347	pFA6a ARS/CEN P(PGK1)-(Ascl)-λN-T2A-SpHIS5	(this study)
pNTI592	pFA6a ARS/CEN RPL28 CaURA3	(this study)
pNTI619	pFA6a ARS/CEN RPL28(exon I)-(Mfe/Nhe) SpHIS5	(this study)
pNTI663	pFA6a ARS/CEN RPL28 SpHIS5	(this study)
pNTI664	pFA6a ARS/CEN RPL28(Q38P) SpHIS5	(this study)
pNTI665	pFA6a ARS/CEN RPL28(H39L) SpHIS5	(this study)
pNTI666	pFA6a ARS/CEN RPL28(K55M) SpHIS5	(this study)

**Supplementary Table 2. Plasmids.** Plasmids used in this study are listed. Annotated plasmid sequences in GenBank record format are available at <https://github.com/ingolia-lab/turbidostat/tree/master/mcgeachy-2018/sequences>. All plasmids are available from Addgene.

## Supplementary Table 3

Strain	Genotype	Source
BY4741 (NIY111)	S288c MATa his3Δ1 leu2Δ0 met15Δ0 ura3Δ0	Invitrogen
NIY414	BY4741 rpl28Δ::KILEU2 pNTI592 (RPL28 CaURA3)	(this study)

**Supplementary Table 3. Yeast strains.** Yeast strains used in this study are listed along with their genotype.